International Journal of Engineering Innovation & Research
Volume 6, Issue 5, ISSN: 2277 – 5668

Using a Confocal Fabry - Perot Interferometer to Analyze the Laser Frequency Stability

Maithya J. Mutuku*, Rurimo G. Kihara and Mutuku J. Ndisya
Jomo Kenyatta University of Agriculture and Technology, Physics Department P.O. Box 62000 (00200), Nairobi, Tel: 0254 067-52711
*Corresponding author email id: maithyajm@yahoo.com

Date of publication (dd/mm/yyyy): 10/09/2017

***Abstract* – The design and fabrication of confocal Fabry perot interferometer (CFPI) is presented. It consists of three parts a central part, a fixed end where a piezo element is fitted and an adjustable end. One of the mirrors is glued to the piezo element and the other mirror is fixed to the adjustable end by use of a Teflon material. A piezo element driven by a triangular wave voltage results in an oscillating movement of the mirror, hence altering slightly the length of the cavity. At resonance a standing wave is formed in the cavity causing an amplified output as the piezo changes the length of the cavity.**

***Keywords* – Confocal Fabry-perot interferometer (CFPI), Driver circuit, Free spectral range (FSR), Laser, Piezo element.**

I. INTRODUCTION

The confocal mirror Fabry-Perot interferometer is a special type of spherical mirror system that uses a pair of concave mirrors whose radii of curvature are equal to their separation, [1], [3] resulting in a common focus. In confocal mirror systems, high finesse is achieved easily for two reasons. First, the focusing of the incident beam reduces possible finesse degradation due to mirror surface imperfections. Second, the common focus of the mirrors results in a simple alignment procedure. The only limitation of a confocal mirror system is that its free spectral range (FSR) is fixed by the radii of curvature of the mirrors [3]-[5]. As the Fabry-Perot interferometer is a very simple device that relies on the interference of multiple beams, it is ideal for measuring laser linewidth, longitudinal mode structure and frequency stability of a laser source. The device consists of two partially transmitting mirrors that are precisely aligned to form a reflective cavity [6]-[8]. Incident light enters the Fabry-Perot cavity and undergoes multiple reflections between the mirrors so that the light can interfere with itself many times [9]. If the frequency of the incident light is such that constructive interference occurs within the Fabry-Perot cavity, the light will be transmitted. Otherwise, destructive interference will not allow any light through the Fabry-Perot interferometer [10], [11]. The condition for constructive interference within a Fabry-Perot interferometer is that the light forms a standing wave between the two mirrors as shown in Figure 1.

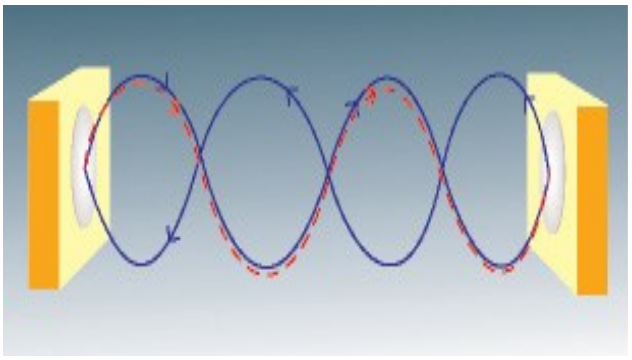

Fig. 1. Standing wave within a Fabry-Perot cavity.

The constructive interference condition therefore is defined by the equation:

$$nd\cos\theta = \frac{m\lambda}{2} \qquad (1)$$

Where m is an integer known as the order of interference, n is the refractive index of the medium between the two mirrors, d is the mirror separation and θ is the inclination of the direction of the incoming radiation to the normal of the mirrors [12]. Because air (n = 1) typically is the medium between most Fabry-Perot mirrors, and the incident light usually is aligned normal to the mirrors (cosθ = 1), the constructive interference equation can be reduced to:

$$d = \frac{m\lambda}{2} \qquad (2)$$

This equation shows that the wavelength transmitted by a Fabry-Perot interferometer depends on the physical separation between the interferometer's mirrors. Therefore, by employing piezoelectric mirror spacers to which a voltage is applied (to smoothly adjust the mirror separation), the transmitted wavelength of a Fabry-Perot interferometer can be tuned precisely to form transmission peaks [13], [14]. The transmission peaks are called fringes. The transmission peaks can be used to monitor the scanning of the laser frequency precisely. The difference in frequency between two fringes is defined as the free spectral range (FSR) of the cavity [15], [16] as seen in figure 3. It depends on the distance between the two mirrors and is given by equation 3.

$$FSR = \frac{c}{2d} \qquad (3)$$

Where c is the velocity of light and d is the mirror separation.

II. EXPERIMENTAL

Fabrication of Confocal Fabry-Perot Interferometer

The cross-section of the Fabry-perot with measurements in mm was done as shown in figure 3.

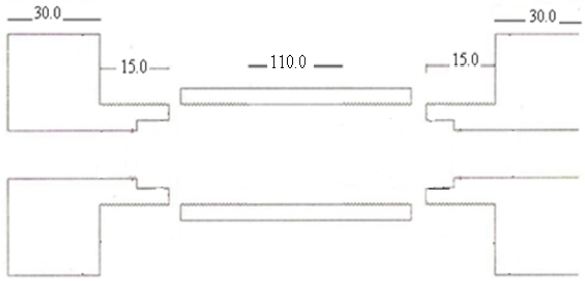

Fig. 3. The cross-section of the Fabry-perot with measurements in mm.

A sketch of the CFPI was done to ensure that the required mirror separation was attained. Measurements of the length of the Piezo element, mirror thickness and the Teflon material thickness were important because they contributed to the distance of separation of the mirrors which corresponded to the confocal point of the CFPI. These measurements led to the sketch on Figure 3 which was used to design the CFPI. A design for the frame of the confocal Fabry-perot interferometer (CFPI) was done as shown in figure 4.

A design for the frame of the confocal Fabry-perot interferometer (CFPI) and initial measurements were then done as shown in figure 4.

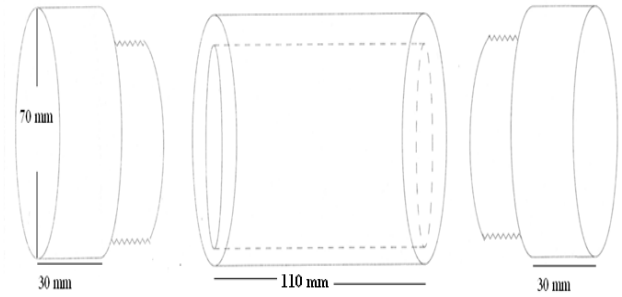

Fig. 4. The design for the frame of the CFPI.

The body of the interferometer was constructed using brass material. Brass is an alloy of copper and zinc, the proportions of zinc and copper can be varied to create a range of brasses with varying properties. Brass was used because it has higher malleability, relatively low melting point (900°C to 940°C depending on composition) and its flow characteristics make it a relatively easy material to cast. Three pieces of brass material were designed, two of equal length 30 mm and diameter 70 mm and one longer which constitutes the central part of the CFPI. The length of the central part was 110 mm and the internal diameter was 33 mm. Threads were made on both sides of the central part material. Two brass materials of equal length and external diameters were designed. One of the ends of each material was reduced in size and threaded to fit into the internal diameter of the central part. The CFPI was designed to have two ends (i.e. the fixed end and the adjustable end) attached to the central part. On the adjustable end a hole of diameter 12.7 mm was drilled carefully at the centre of the threaded end to fit a mirror by use of a Teflon material fixed to the brass using screws. Adjustments of the mirror separation of the CFPI were done on this end i.e. mirror separation. The hole on the fixed end was 12.0 mm in size, the piezo element with external diameter 14 mm glued to a mirror was fitted to this hole by a Teflon material of thickness 5.5 mm and diameter 30 mm.

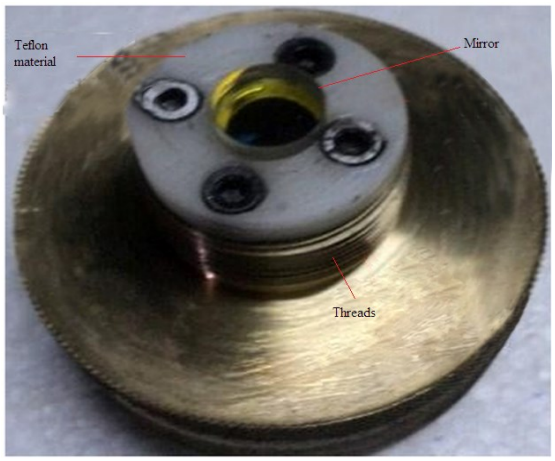

Plate 1: A mirror glued to the adjustable end.

One of the standard concave mirrors was fitted by use of a Teflon material directly to the adjustable end using screws as shown in plate 1. The adjustable end is used to vary the separation distance between the two mirrors. The Teflon material was used to fix the mirror to the brass material.

Plate 2 shows the central part of the body of CFPI were the fixed end and the adjustable ends are fitted. The CFPI is supported by the stand at this part.

Plate 2: Central part of the CFPI.

Plate 3 shows the internal part of the fixed end with a hole drilled to fit the piezo element and other two holes drilled appropriately for the piezo leads to pass through to the outer side.

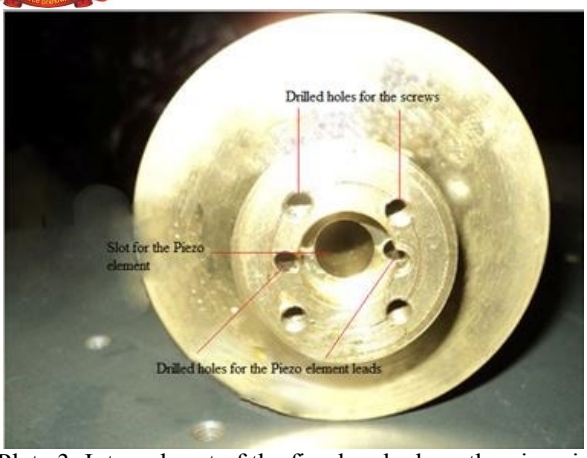

Plate 3: Internal part of the fixed end where the piezo is slotted.

The second identical mirror was glued to the piezo element, which in turn, was fitted using Teflon material to the second metal pipe by screws as shown in plate 4.

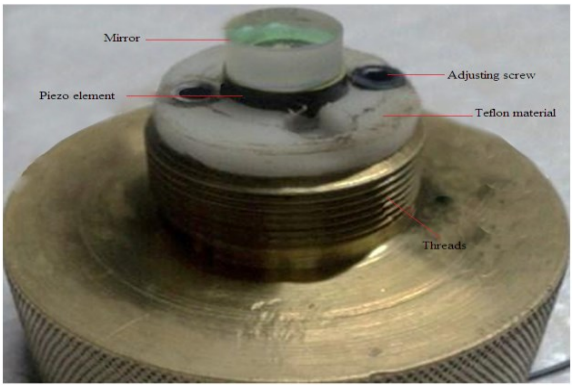

Plate 4: Piezo element with a mirror glued to the fixed end.

This end is adjusted and its position maintained. The leads connected to the piezo element are grooved through the body of the mount. This is to ensure that the leads don't block the laser beam ensuring that the beam reaches the mirror attached to the piezo without interference as shown in plate 5.

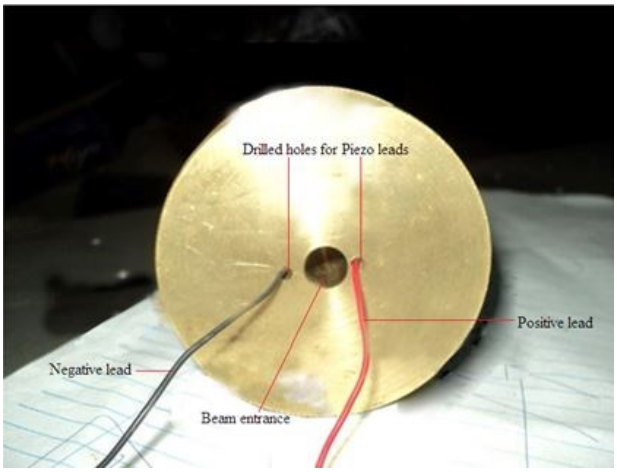

Plate 5: Rear part of the fixed end with the piezo leads emerging.

The beam from a He-Ne laser enters the CFPI through this hole of diameter 10 mm drilled at the centre of the fixed end and leaves through another hole of the same diameter on the adjustable end. When the beam emerges on the adjustable end it is received by a photodiode on the photo detector circuit. A confocal Fabry-perot interferometer was designed and fabricated as shown in plate 6.

Plate 6 shows a complete frame for the confocal Fabry-perot interferometer. The body of the CFPI was made rough to ensure there was good grip when adjustments were being made.

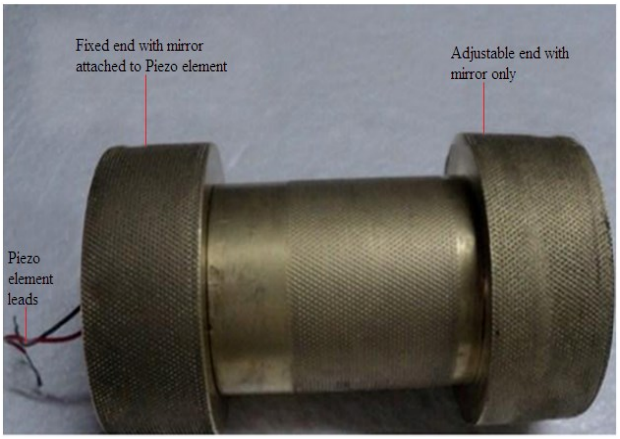

Plate 6: Complete frame for the confocal Fabry-perot interferometer.

CFP Mounting

The interferometer mount holds the Fabry-Perot interferometer and allows adjustments to precisely align the input laser beam for optimum performance. Aligning the laser beam to the optical axis of the interferometer is critical to ensure that the transmission properties of the interferometer do not depend on any angular effects. The design of the interferometer mount is the key to convenient adjustments and high quality results as shown in plate 7.

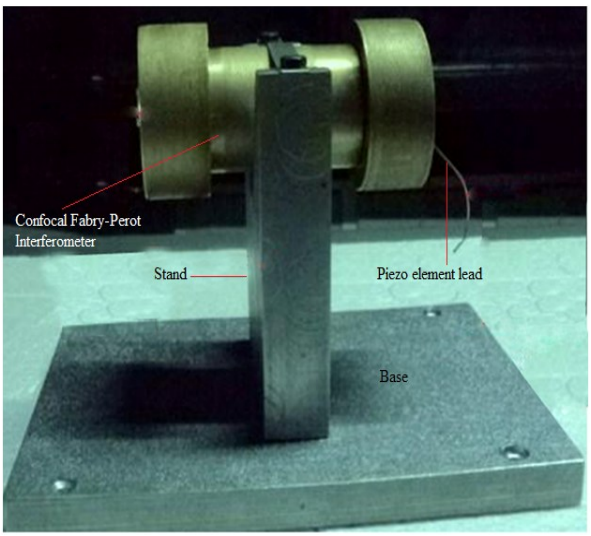

Plate 7: A photograph of the Confocal Fabry-perot interferometer set up.

The stand has a V-groove for slotting the Fabry-perot hence ensuring that the CFPI is firmly held on the stand. The stand has an aluminium strap fitted by use of screws at the top. Once the CFPI is placed on the groove the strap is tightened by the screws holding the CFPI firmly. The bottom of the stand has two holes drilled equidistant from the ends. The dimensions of the stand were 250 mm x 170 mm x 19 mm. The stand is fitted to the base by use of screws which are countersinked to ensure that the base remains flat to fit well on the optical table. The base has holes drilled appropriately so as to be screwed on the optical table. The dimensions of the base were 125 mm x 104 mm x 30 mm. The base was fitted to the optical table using 'M6' screws. The stand and the base were made from aluminium blocks. The base and the stand provided stability to the confocal Fabry-perot interferometer (CFPI) and was crucial for correct alignment.

III. Results and Discussion

One end of the confocal Fabry-perot interferometer is adjustable. During adjustment different distances of mirror separation were obtained which corresponds to a certain beam waist. Distance of separation of the mirrors was selected between 30 mm and 70 mm since the radius of curvature of the mirrors is 50 mm which gives the confocal condition. A table of distance of separation and the corresponding values of the beam waist was generated using equation 4 as shown in table 1.

$$\omega_0^{\,2} = \frac{\lambda}{2\pi}\sqrt{d(2R-d)} \qquad (4)$$

Where

ω_0 - Beam waist.

λ - Wavelength of the laser beam.

d - Distance of separation of the mirrors.

R - Radius of curvature of the mirrors.

The beam parameters R and ω describe the modes of all orders. R is equal to the radius of curvature of the mirrors, which means that the mirror surfaces are coincident with the phase fronts of the resonator modes. d is a variable that is the distance of separation of the mirrors is from 3.0 cm to 7.0 cm. Using equation above the values of d were substituted and corresponding values ω_0 of generated. The distances of separation of the mirrors chosen were points below and above the confocal point of the mirrors. The idea was to establish the behavior of the curve below and above the point.

Table 2. A table of generated values of d and ω_0

d(m) $*10^{-2}$	$\omega_{0} * 10^{-5}$
3.0	6.794
3.2	6.855
3.4	6.908
3.6	6.953
3.8	6.992
4.0	7.025
4.2	7.051
4.4	7.071
4.6	7.086
4.8	7.094
5.0	7.097
5.2	7.094
5.4	7.086
5.6	7.071
5.8	7.051
6.0	7.025
6.2	6.992
6.4	6.953
6.6	6.908
6.8	6.855
7.0	6.794

A graph of ω_0 (beam waist) against the distance of separation of the mirrors was plotted, using the values in table 2 and is as shown in figure 5.

A graph of beam waist (w_0) against distance of separation of mirrors (d).

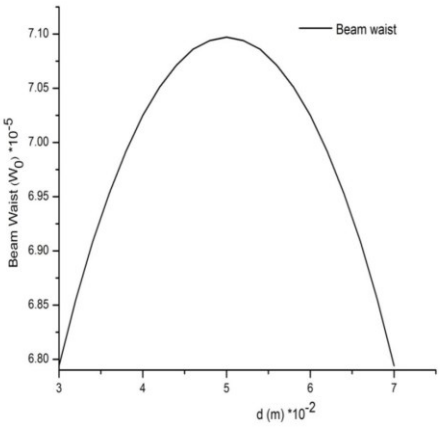

Fig. 5. A plot of beam waist against distance of separation.

The maximum point of the curve corresponds to the confocal condition of a Fabry-perot interferometer. This point can be used to determine the frequency stability of a laser beam. At confocal condition maximum beam waist is attained because all the available modes are in resonance. Below and above this point is the non-confocal of a Fabry-perot interferometer which can be used to spatially filter unwanted modes in laser beam in order to meet the stringent requirements of a diffraction limited beam demanded by most optical experiments.

Measuring Confocal Cavity Characteristics

The adjustable end of the confocal Fabry-perot interferometer was adjusted mechanically. Measurements of the output beam when the piezo driver circuit was switched off were taken before the confocal point, at the confocal point and after the confocal point. The following photographs were obtained before the confocal point, at the confocal point and after the confocal point.

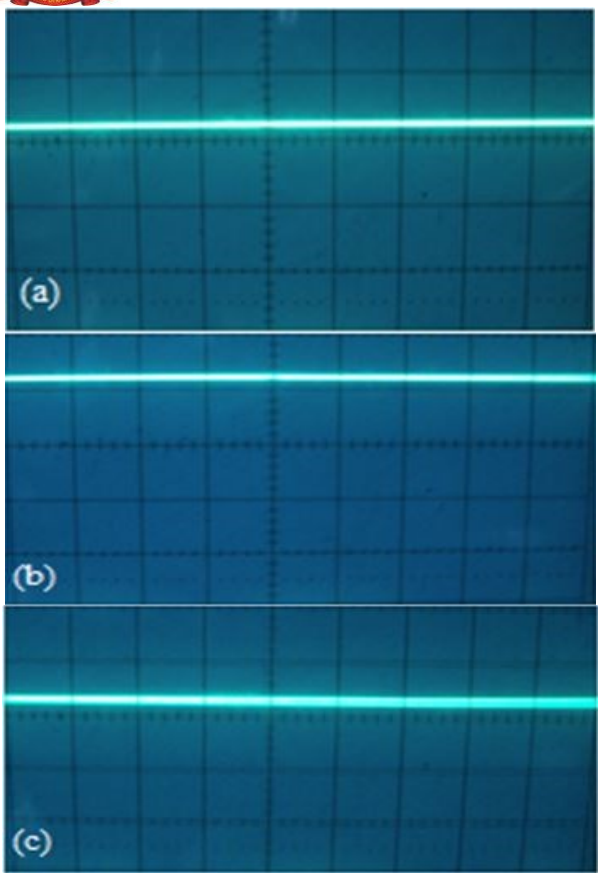

Plate 8: A photograph of the output signal when the Piezo driver circuit was switched off and the cavity length manually adjusted.

Plate 8 shows the output signal from the Fabry-perot when the cavity length was manually adjusted, (a) at approximately 8 mm before the confocal point was reached (b) at the confocal point and (c) at approximately 10 mm after the confocal point. At the confocal point the output signal increases as shown in the plate (b) because the resonance condition has been attained.

As the adjustments on the CFPI continued, different transmission fringes were observed on the oscilloscope. This is because the piezo element expands when subjected to a voltage hence altering slightly the length of the cavity. At some point during the adjustments the transmission fringe increased to a maximum (amplified output) and after that point decreased to a minimum. The maximum transmission peak was obtained at the confocal point. This implies that, at this point the resonance condition of the CFPI was attained. At resonance a standing wave is formed in the cavity causing an amplified output. The maximum transmission peak implies that the transmitted beams are in phase and therefore constructive interference occurs. If the transmitted beams are out of phase destructive interference occurs and this corresponds to a transmission minimum. The output beam from the CFPI was directed to the photodiode in the photo detector circuit and the results displayed on an oscilloscope. When the output beam from the CFPI falls on the photodiode, photocurrent is generated which is converted to voltage.

The Confocal Measurements

When the piezo driver circuit was switched on measurements of the output beam were made at the confocal point at different times. The following photographs were obtained at resonance condition from the oscilloscope. Plate 9 (a) was taken immediately the laser was switched on, plate 9 (b) after one hour, plate 10 (a) after two hours, plate 10 (b) after 3 hours, plate 11 (a) after 4 hours and plate 11 (b) after 5 hours.

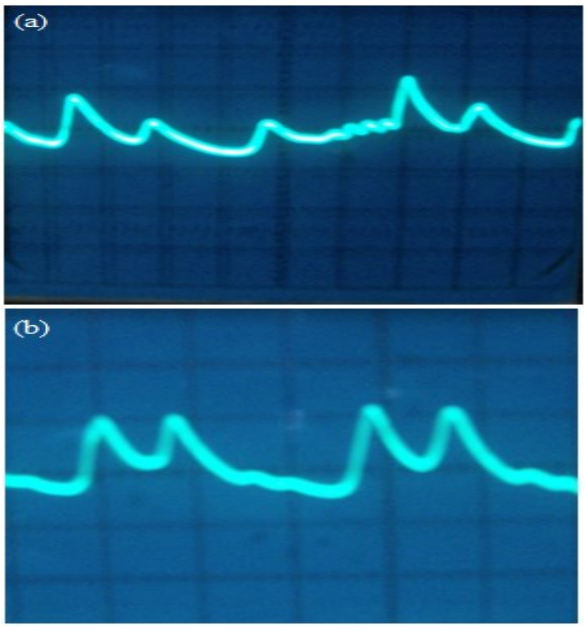

Plate 9 (a): A photograph of the oscilloscope screen showing the Fabry-perot output immediately the Laser was switched on. (b) the Fabry-perot output after the Laser has been running for 1 hour. The piezo driving frequency was set at 150 Hz.

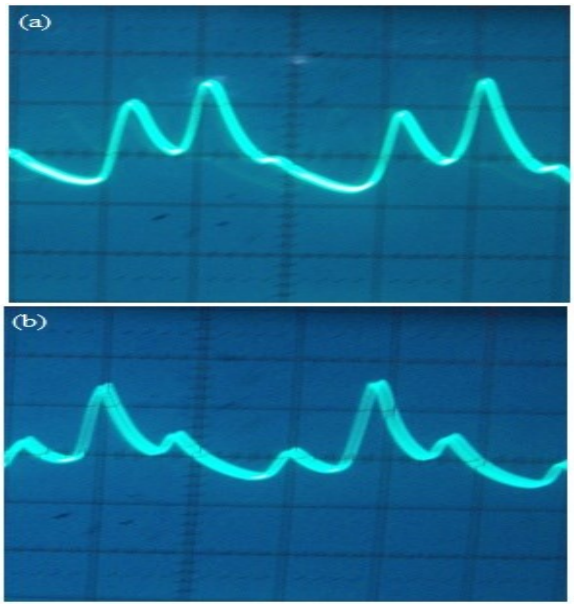

Plate 10 (a): A photograph of the oscilloscope screen showing the Fabry-perot output after the Laser has been running for 2 hours (b) the Fabry-perot output after the Laser has been running for 3 hours. The piezo driving frequency was set at 150 Hz.

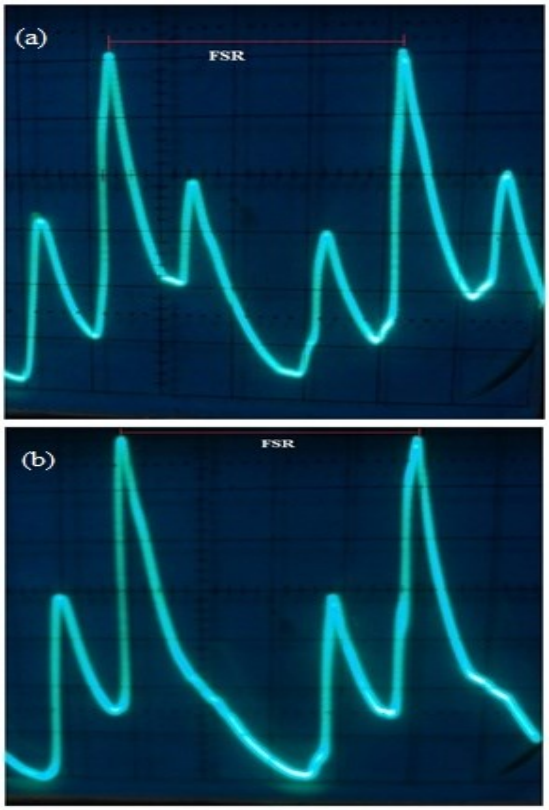

Plate 11(a): A photograph of the oscilloscope screen showing the Fabry-perot output after the Laser has been running for 4 hours (b) the Fabry-perot output after the Laser has been running for 5 hours. The piezo driving frequency was set at 150 Hz.

Plate 12 and plate 14 shows the Oscillogram of the signal from the photodetector. Plates 12 and 13 were taken after the laser had been left to run for 4 hours while plates 14 and plate 15 were taken after 5 hours implying that the laser stabilizes after 5 hours. The results of the He-Ne laser with power of 10 mW and wavelength 632.8 nm from Thorlabs are as shown in the plates below.

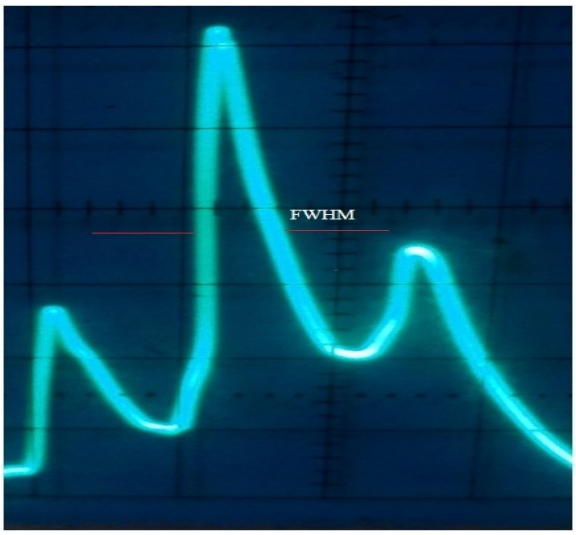

Plate 12: A photograph of the Oscillogram of the signal from the photodetector with Piezo driving frequency of 100 Hz.

The laser is running on three modes; a central mode, one on the right hand side formed at 5.5 ms and the other one on the left hand side at 3.1 ms. One big square of the oscilloscope represents 1 ms. The differences in time of the two modes from the central mode were calculated as follows:

Central mode is formed at 4.3 ms from the zero reference of the oscilloscope.

Mode on the left hand side = 3.1 ms.

The difference = 4.3 ms – 3.1 ms.

= 1.2 ms.

Mode on the right hand side = 5.5 ms.

The difference = 5.5 ms – 4.3 ms.

=1.2 ms.

When the laser stabilises and fine tuning the CFPI, the competing mode on the right hand side of the main mode loses its power to the main mode hence increasing the peak of the main mode meaning more power as shown in plate 14.

The full width at half maximum = 4.7 ms – 4.1 ms

= 0.6 ms

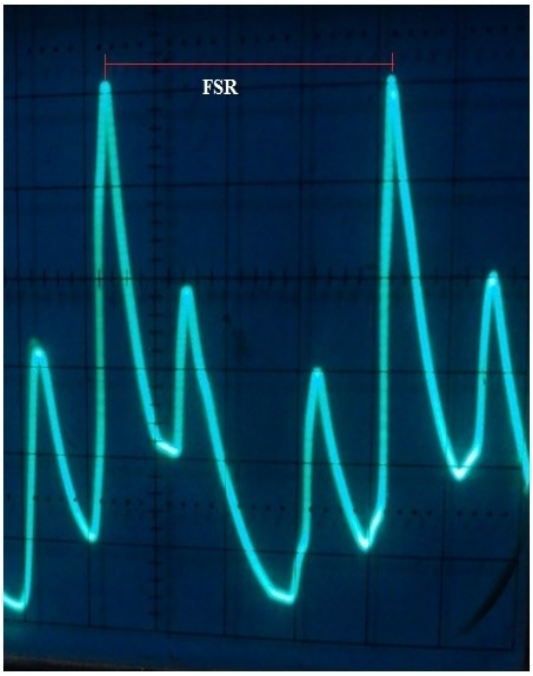

Plate 13: A photograph of the Oscilloscope screen of the free spectral range calculation for the confocal cavity with Piezo driving frequency of 150 Hz.

Δt = 8.3 ms – 4.3 ms

= 4.0 ms

Δt calculated above corresponds to the Free Spectral Range for the confocal cavity.

The maximum transmission peak in plate 12 is not symmetrical due to the competing mode on the right. The results of plates 12 and plate 14 were obtained with the piezo frequency set at 100 Hz and the time base on the oscilloscope set at 1 ms/Division, while those for plate 13 the piezo frequency was set at 150 Hz.

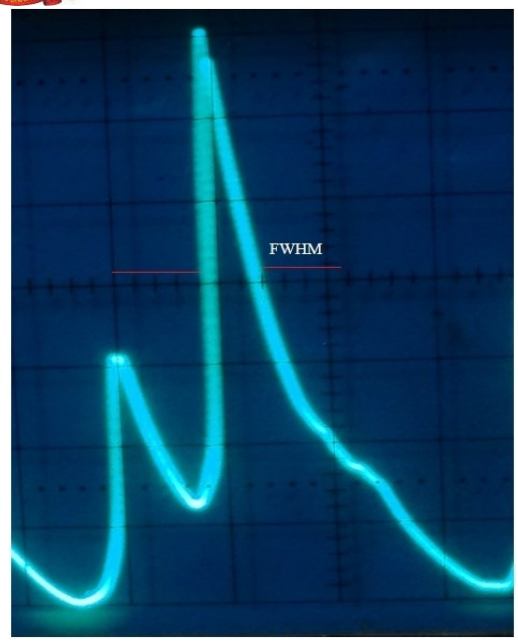

Plate 14: A photograph of the Oscillogram of the signal from the photodetector with Piezo driving frequency of 100 Hz.

The full width at half maximum = 4.4ms – 3.8ms
= 0.6 ms

The two transmission peaks in plates 13 and 15 were obtained with the piezo frequency set at 150 Hz and the time base on the oscilloscope set at 1 ms/Division. When the frequency is increased the rate of scanning also increases.

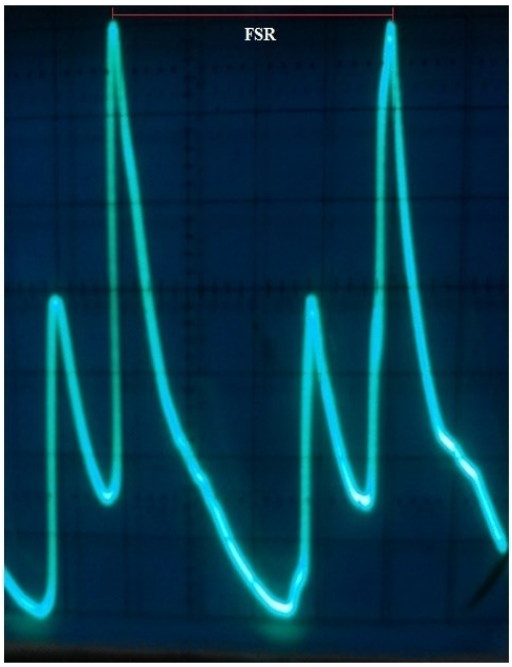

Plate 15: A photograph of the Oscilloscope screen of the free spectral range calculation for the confocal cavity with Piezo driving frequency of 150 Hz.

Δt = 7.9ms – 3.9 ms
= 4.0 ms

Plates 13 and 15 show the free spectral range for the cavity. It was obtained by changing the time base on the oscilloscope. The two transmission peaks (fringes) were obtained by reducing the time base on the oscilloscope thereby increasing the frequency. The side bands were due to a competing mode present on the beam.

The Free Spectral Range of the confocal cavity was calculated using equation (3). The line width is then calculated by dividing the free spectral range by the finesse. The confocal cavity was found to have a free spectral range of 3.0 MHz, a finesse of 61.24 and the line width to be 0.049 MHz. The pitch of the adjustable end was 1.5 mm and therefore for one to get good results it has to be reduced since it affects the distance of separation of the mirrors. It was also important to determine some characteristics of the mirrors. The reflectance of the cavity mirrors is 95 ± 0.5% and transmittance is 4.9149%.

Finesse is a function of reflectivity. The higher the reflectivity the higher the finesse. A higher finesse value indicates a greater number of interfering beams, which results in a more complete interference process and therefore higher resolution measurements. Other parameters for the CFPI were evaluated. Maximum order of interference occurs when the beam is perpendicular to the reflecting surface of the mirror. The confocal cavity was found to have a maximum order of interference of approximately 1.58 x 10^5, maximum resolvable wavelength of 3.26 x 10^{-4} nm and resolving power of 1.94 x 10^6.

IV. Conclusion

It was observed that the He-Ne laser had another mode very close to the dominant wavelength when switched on. In many applications, it is necessary to know how many modes are oscillating, it may even be necessary to limit the number of modes that are oscillating in the laser. For example, in holography, several modes oscillating simultaneously in a laser limit the coherence length of the laser beam and, thus, limit the depth of field of the hologram made with the laser. To limit the number of modes oscillating in a laser the Fabry-perot interferometer was used. A confocal Fabry-Perot interferometer was designed and implemented with one of the mirrors glued to the piezo element and fitted into the fixed end and the other mirror to the adjustable end of the CFPI by use of a Teflon material. The confocal cavity was found to have a free spectral range of 3.0 MHz, a finesse of 61.24 and the line width of 0.049 MHz. The reflectance of the cavity mirrors is 95 ± 0.5% and transmittance is 4.9149%.

Table 1. Distance of separation of the mirrors and the corresponding values of ω_0

d (m)	$\lambda/2\pi$	2R-d	d(2R-d)	□ (d(2R-d))	$\omega_0^2 * 10^{-9}$	$\omega_0 * 10^{-5}$
0.03	1.0073201782E-07	0.070	0.00210	0.0458258	4.61612	6.794204
0.032	1.0073201782E-07	0.068	0.00218	0.0466476	4.69891	6.854858
0.034	1.0073201782E-07	0.066	0.00224	0.0473709	4.77176	6.907796
0.036	1.0073201782E-07	0.064	0.00230	0.048	4.83514	6.953515
0.038	1.0073201782E-07	0.062	0.00236	0.0485386	4.88940	6.992421
0.04	1.0073201782E-07	0.060	0.00240	0.0489898	4.93484	7.024842
0.042	1.0073201782E-07	0.058	0.00244	0.0493559	4.97171	7.051039

d (m)	λ/2π	2R-d	d(2R-d)	□ (d(2R-d))	$\omega_0^2 * 10^{-9}$	$\omega_0 * 10^{-5}$
0.044	1.0073201782E-07	0.056	0.00246	0.0496387	5.00021	7.071213
0.046	1.0073201782E-07	0.054	0.00248	0.0498397	5.02046	7.085519
0.048	1.0073201782E-07	0.052	0.00250	0.04996	5.03257	7.094061
0.05	1.0073201782E-07	0.050	0.00250	0.05	5.03660	7.096901
0.052	1.0073201782E-07	0.048	0.00250	0.04996	5.03257	7.094061
0.054	1.0073201782E-07	0.046	0.00248	0.0498397	5.02046	7.085519
0.056	1.0073201782E-07	0.044	0.00246	0.0496387	5.00021	7.071213
0.058	1.0073201782E-07	0.042	0.00244	0.0493559	4.97171	7.051039
0.06	1.0073201782E-07	0.040	0.00240	0.0489898	4.93484	7.024842
0.062	1.0073201782E-07	0.038	0.00236	0.0485386	4.88940	6.992421
0.064	1.0073201782E-07	0.036	0.00230	0.048	4.83514	6.953515
0.066	1.0073201782E-07	0.034	0.00224	0.0473709	4.77176	6.907796
0.068	1.0073201782E-07	0.032	0.00218	0.0466476	4.69891	6.854858
0.07	1.0073201782E-07	0.03	0.0021	0.0458258	4.61612	6.794204

REFERENCES

[1] Richard, L. Bryon, and A. Charles, "Mode power partition events in nearly single-frequency lasers, *Journal of light wave Technology*," vol. 3, 1985, pp.7066-7711.
[2] Sasaki, K. Wakabayashi, and S. Masuda, "Stabilization of single frequency internal mirror He-Ne Lasers, *Applied Optics,"* vol. 28, 1989, pp. 1608-1609
[3] Babbitt, W. and Mossberg, T. (1995) ''Spatial routing of optical beams through time-domain spatial-spectral filtering,'' *Optics Letters* 20, 910.
[4] Bishnu, P. (2005). Fundamentals of fibre optics in telecommunication and sensor systems. Delhi: New Age International Ltd. publishers. 663-669.
[5] Born, E. (1975). Principles of optics, Pergamon press, Oxford, 127-130
[6] J. James, and R. Sternberg, (1969). The design of optical Spectrometers, Chapman and Hall Ltd, London, 420-428.
[7] J. Sandercock, "Simple stabilization scheme for maintenance of alignment in a scanning Fabry-perot interferometer, *Journal of physics,"* vol. 9, 1976, pp. 566-570
[8] J.B. Pawley, *Hand book of Biological confocal microscopy*. New York: Plenum Press, 1998, pp. 120 -127.
[9] J.M. Hollas, *Modern Spectroscopy*. London: John Wiley, 1988, pp. 306-309.
[10] L. Frank, and S. Leno, *Introduction to optics*. New Jersey: Prentice-Hall, Inc., 1993, pp. 239-244.
[11] M. Hercher, "The spherical mirror Fabry-Perot interferometer," *Applied Optics*, Vol.7, 1968, pp. 951-966.
[12] P. Ciddor, and M. Duffy, "Two-mode frequency-stabilized He-Ne (633 nm) Lasers: Studies of short- and long- Term stability, *Journal of physics,*" vol.16, 1983, pp. 1223-1227.
[13] P. Herre and U. Barabas, "Mode switching of Fabry-perot laser diodes, *IEEE journal of Quantum electronics*," vol.25, 1989, pp. 1790-1794.
[14] R. Balhorn, H. Kunzmann, and F. Lebowsky, "Frequency stabilization of internal mirror Helium-Neon Lasers, *Applied Optics,*" vol.11, 1972, pp. 742-744.
[15] R. George, and R. Rajarshi, "Bistability and mode hopping in a semiconductor laser, *Journal of the optical society of America*," vol. 8, 1991, pp. 632-638.
[16] W. Demtröder, *Laser spectroscopy, Basic concepts and instrumentation*. Berlin Heidelberg: Springer-Verlag, 2003, pp. 23- 46.

AUTHORS' PROFILES

Mr. Justus M. Maithya is a Tutorial Fellow in Physics Department at JKUAT. He has a Master's Degree in Physics specializing in Electronics and Optics from Jomo Kenyatta University of Agriculture and Technology. He is currently doing his PhD in Graduate School of Engineering, Department of Earth Resource Engineering at Kyushu University in Japan.
E-mail: maithyajm@yahoo.com

Dr. Joseph N. Mutuku is an Associate Professor in Physics Department at JKUAT. He has been actively involved in teaching and research in the fields of Digital Electronics and Microprocessors, Instrumentation and Electrical properties of Polymer materials. He has published widely in international peer reviewed journals.
E-mail: jmndisya@yahoo.com

Dr. Geoffrey K. Rurimo is an Associate Professor in Physics Department at JKUAT. He has been actively involved in research and teaching at both undergraduate and postgraduate levels in Optics and Lasers. He studied his PhD at Max-Planck Institute for the Science of Light in the Institute of Optics, Information and Photonics, University of Erlangen, Germany. He has published widely in international peer reviewed journals.
Email address: grurimo@gmail.com